

NOISE REDUCTION IN TERAHERTZ THIN FILM MEASUREMENTS USING A DOUBLE MODULATED DIFFERENTIAL TECHNIQUE

SAMUEL P. MICKAN* and DEREK ABBOTT†

*Centre for Biomedical Engineering (CBME),
Department of Electrical & Electronic Engineering,
Adelaide University SA 5005, Australia*
*spmickan@eleceng.adelaide.edu.au
†dabbott@eleceng.adelaide.edu.au

JESPER MUNCH

*Department of Physics & Mathematical Physics,
Adelaide University SA 5005, Australia*
jmunch@physics.adelaide.edu.au

X.-C. ZHANG

*Department of Physics, Applied Physics & Astronomy,
Department of Electrical & Electronic Engineering,
Rensselaer Polytechnic Institute, Troy NY 12180, USA*
zhangxc@rpi.edu

Received 4 February 2002

Revised 25 March 2002

Accepted 2 April 2002

Differential terahertz (THz) time-domain spectroscopy (TDS) is a technique for decreasing noise levels in THz thin film characterization experiments. Characterizing thin films in the GHz to THz range is critical for the development of fast integrated circuits and photonic systems, and is potentially applicable to biosensors and proteomics. This paper shows how the differential technique, combined with double modulation, enables the study of thin films with noise reduction over normal TDS that improves as the film gets thinner. Double modulated differential THz-TDS has enabled the characterization of films with less than 1- μm thickness.

Keywords: Terahertz; spectroscopy; double modulation; thin films.

1. Introduction

This paper reviews the background of THz technology development, and considers the problem of thin film characterization with THz. A proposed solution to the thin film characterization problem is differential THz time-domain spectroscopy

(DTDS), which has been recently described in [1]. This work presents a detailed noise analysis of DTDS and shows, theoretically and experimentally, the benefits of using DTDS with double modulation. We conclude by summarizing our results and discussing the future directions of our work.

1.1. *Motivation*

Thin film characterization is a fundamental problem in optics and electronics. Terahertz time-domain spectroscopy (THz-TDS) is a technique developed in the last decade for characterizing samples in the THz band of the electro-magnetic spectrum. THz-TDS provides a new non-destructive method for probing thin films at speeds higher than network analyzers and wavelengths longer than optical sources. The high noise background associated with THz-TDS of very thin samples can be vastly improved by using differential THz-TDS (DTDS) and a scheme of double modulation.

Thin film characterization is important for the semiconductor industry as it pushes for smaller and faster devices. Materials with a high dielectric constant are required for improved insulation to stop tunneling between layers, and materials with a low dielectric are needed for interconnects with reduced capacitance [2]. As feature sizes approach 100 nm and chip frequencies climb into the upper gigahertz range, it becomes increasingly important to have a convenient method of characterizing the THz properties of thin dielectric films [3]. Thin film dielectric materials are being explored for many applications. Interest in plastic-based electronics is spurring the development of organic-inorganic hybrid materials and organic transistors on plastic [4,5]. Single crystal optoelectronic devices are being developed for thin film transistors and MOEMS [6].

THz systems are non-contact, non-destructive and highly sensitive. Apart from applications in high speed device characterization, THz radiation has been used for sensitive quality control, chemical spectroscopy and biomedical diagnostics. THz penetrates optically opaque materials that cannot be characterized using optical methods, and can be used in transmission, reflection and tomographic experiments [7]. THz has the potential to become a widespread diagnostic tool in the future.

1.2. *THz-TDS*

THz (10^{12} Hz, $\lambda = 0.3$ mm) frequency radiation has historically been difficult to generate and detect [8]. Thermal sources have weak emission at long wavelengths and gas vapor lasers are cumbersome [9]. Bolometric detectors only operate under vacuum at liquid-helium temperatures [10]. Fourier Transform Infrared (FTIR) spectroscopy does offer spectroscopic information down to about 1 THz, but not into the GHz regime [11]. Research continues into many sources and detectors in the THz band, including germanium lasers, gas-vapor lasers, quantum cascade lasers and backward-wave oscillators [12–15].

The development of pulsed THz radiation (T-rays) generated using ultrafast optical lasers has provided a new method for accessing the THz frequency regime. Pulsed THz techniques were initially developed for waveguides and circuit characterization [16–18]. Free-space THz spectroscopy grew from the development of both photoconductive dipole antennas and electro-optic crystals as sources and

detectors [19–22]. The spectroscopy of bulk dielectrics at THz frequencies was part of the early work in the field [23, 24].

Recent developments in T-ray research are wide-reaching. T-rays have been extended to two-dimensional and three-dimensional imaging using a variety of scanning and CCD techniques [25–30]. T-ray spatial resolution has been improved by the development of near field imaging [31–33]. T-ray systems now exhibit very high signal-to-noise ratios and are being implemented in applications ranging from scaled-down “radar” profiling and cancer detection [34–36].

2. Problem: THz-TDS of Thin Films

There is a need for a non-contact, room temperature technique to characterize thin films at THz frequencies. Current methods of dielectric thin film characterization show a gap in information from 0.144 to 5 THz [37]. This gap is covered by the typical operating bandwidth of T-ray systems.

Thin film analysis is limited by system sensitivity; the thickness of a thin film, being microns or less, is far less than the T-ray wavelength. A number of approaches have been used to increase system sensitivity, including DTDS, angle-dependend spectroscopy, interferometry and planar waveguides.

The complex dielectric constant of a sample is related to its optical properties by the relation $\tilde{\epsilon} = (\tilde{n})^2$, where, for extinction coefficient κ and refractive index n , $\tilde{n} = n - j\kappa$.

The phase shift caused by a dielectric sample in the T-ray radiation path is proportional to $(\tilde{n} - 1)d/\lambda$, where \tilde{n} is the complex refractive index of the medium, d is the sample thickness and λ is the T-ray wavelength [35]. For small \tilde{n} and d , this phase change is very difficult to detect in background noise.

T-rays have been used to characterize a wide variety of thin film materials using different techniques. T-rays can be used to observe static and dynamic characteristics of superconducting films, dielectrics in waveguides and DNA thin films [38–41]. Organic thin polymer films were first characterized by T-rays in 1992 [42]. A reliable algorithm for estimating the T-ray characteristics of thin film dielectrics was proposed in 1996 [43]. This method uses a model based on simple Fresnel equations and an iterative fit algorithm. Near-Brewster angle (“goniometric”) phase shift reflection has been used to determine the refractive index of 3.27- μm -thick polymer films [37]. An incorporation of this technique into tomography has been suggested by angle-dependend T-ray tomography of thin films for fuel cell applications [7].

T-ray interferometry is another method to increase the sensitivity of the T-ray system. T-ray interferometric techniques typically induce a 180° (Gouy) phase shift in one arm of a Michelson interferometer, then detect phase changes introduced by a thin sample into one arm. Enhanced depth and spatial resolution have been achieved with T-rays focused to a point on a reflective sample in one arm of an interferometer, where the Gouy shift occurs at the focal point on the sample [48]. The peak amplitude showed a 20% change for a 12.5- μm -thick air gap in Teflon. Another interferometer has been constructed using silicon prisms as reflectors, where a 180° phase shift was induced by a fixed end reflection from one of the faces [49]. This study characterized the real and imaginary parts of the refractive index of a 2- μm -thick film of free-standing Mylar.

Using planar waveguides and a THz resonator, Bolivar *et al.* have demonstrated a highly sensitive device for probing the binding state of DNA [50]. This thin film micro-stripline approach can be extended to two-dimensional gene chips for high speed DNA analysis. The THz waveguide and resonator structure is sensitive to single-base defects in a 1.1 femtomol volume of 0.52 g/L DNA-in-water. Although highly sensitive and integrable, this technique is not ideal for non-contact characterization of thin dielectric films.

The techniques described above have achieved spectroscopy and imaging of dielectrics of micron thickness. The challenge remains, however, to extend T-ray frequency characterization to thinner films and lower dielectric constants. A promising technique for further improving T-ray system sensitivity is DTDS.

3. Proposed Solution: Double Modulated DTDS

The problem of detecting the small signal from absorption, reflection and delay in a thin film can be solved by using what has been called *differential THz time-domain spectroscopy* [51] or ultra-high sensitivity spectroscopy [52]. DTDS measures a signal that comes purely from the difference caused by a thin film deposited on half of a sample holder; the other half is used as a reference. DTDS measures only the difference between the two halves every 100 ms or less, thereby canceling out slow fluctuations in the laser power, which is the main source of noise. Although terahertz is high frequency radiation (10^{12}), it is detected by sampling the ultrafast pulse on a timescale that corresponds to ms or longer [53]. Unfortunately, the samples cannot be physically switched at very high frequencies, which removes the benefit of high frequency modulation with an optical chopper. Double modulation combines the benefits of both to provide a reduced noise over both normal DTDS and high-frequency-modulated THz-TDS.

3.1. *Differential THz time-domain spectroscopy (DTDS)*

The advantage of DTDS is to modulate the T-ray signal using only the thin film, and detect the magnitude of this modulation using a lock-in amplifier (LIA). The sample is a substrate half-covered with the film and half bare, as shown in Fig. 1a.

DTDS is able to measure very subtle variations in phase and absorption. In a normal THz-TDS experiment, this difference is determined from the ratio of two complex spectra, $\tilde{S}_{\text{film}}/\tilde{S}_{\text{ref}}$, where the complex spectral components \tilde{S} are the Fourier Transforms of the time domain waveforms measured in the experiment. Each waveform is measured in a separate scan of the pump beam delay stage, resulting in a delay between scans of ten minutes or more for sensitive scans. For a typical T-ray system, the major source of noise is the pump laser, which is very sensitive to slow fluctuations in temperature. These fluctuations can cause larger changes in the detected T-ray signal than the thin film sample itself. The advantage of DTDS is that the signal transmitted through the film is compared to the signal through the substrate at each point of the delay stage. In effect, the differential waveform is equivalent to the difference between the reference and sample waveforms, $y_{\text{diff}} = y_{\text{ref}} - y_{\text{film}}$.

The benefit of using DTDS over THz-TDS for characterizing thin films can be estimated using a simple analysis of measurement error in the amplitude spectrum,

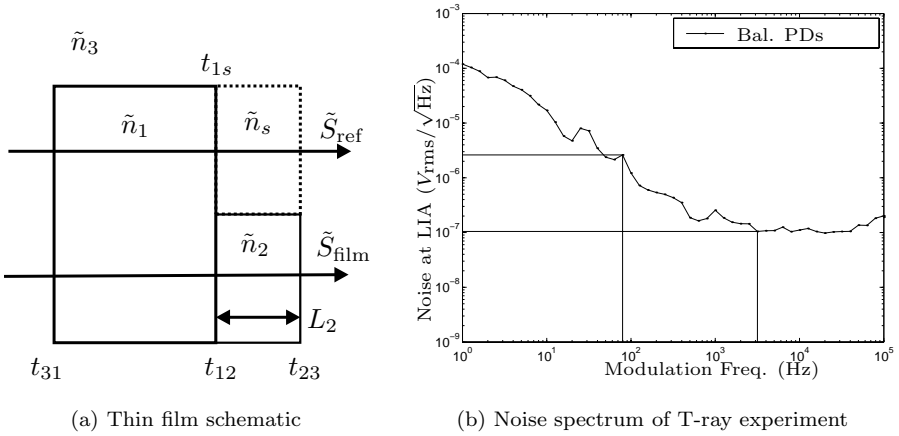


Fig. 1. (a) shows the schematic of a thin film sample prepared for DTDS. The thin film, characterized by the complex refractive index \tilde{n}_2 , is supported by a substrate, \tilde{n}_1 . The surrounding medium, in our case air, has the complex refractive index \tilde{n}_3 . \tilde{n}_s is the complex refractive index of the medium that replaces the volume of the thin film — in our experiments this is air, although if the thin layer is created by implantation of the substrate, \tilde{n}_s may differ from \tilde{n}_3 . For example, if a layer of \tilde{n}_2 is created by implanting a dopant into a silicon substrate, \tilde{n}_1 , then the \tilde{n}_s layer would be silicon not air. The spectral components that are transmitted through the substrate are denoted by \tilde{S}_{ref} and the components transmitted through the substrate and the film are denoted \tilde{S}_{film} . L_2 is the thickness of the thin film, measured using, for example, atomic force microscopy. The Fresnel transmission coefficients, t_{ab} , indicate the transmission from medium a to medium b , where $t_{ab} = 2\tilde{n}_a/(\tilde{n}_a + \tilde{n}_b)$. In DTDS, the signal is made up of the difference between \tilde{S}_{ref} and \tilde{S}_{film} by rapidly switching between them. (b) shows the noise spectrum of our T-ray system with balanced photodiodes (PDs) versus the modulation frequency used with the lock-in amplifier. The noise spectrum shows an $1/f$ noise characteristic typical of ultrafast laser-driven experiments [44–47]. The benefit of double modulation is highlighted by the two lines at 100 Hz and 3 kHz. The noise level at 3 kHz and above is more than an order of magnitude lower than the noise at 100 Hz and below. The noise spectrum was measured using biased PDs, a 50- Ω load impedance and a LIA swept through different frequencies. The noise output of the LIA was measured with a settling time of 60 times the time constant.

that is errors arising from $\Delta|\tilde{S}| = \Delta S$. Analysis of phase error will be considered in future work.

The quantity of interest in dielectric characterization experiments is the deconvolved system response, or the transmission spectrum,

$$T(\omega) = \frac{S_f(\omega)}{S_r(\omega)}, \quad (1)$$

where S_f and S_r are the amplitudes of the spectral components of the film (sample) and reference waveforms. For nominally uncorrelated measurement errors of the amplitude spectra ΔS_f and ΔS_r , the relative error in the amplitude transmission spectrum can thus be approximated by

$$\left(\frac{\Delta T}{T}\right)_{\text{TDS}}^2 \approx \left(\frac{\Delta S_f}{S_f}\right)^2 + \left(\frac{\Delta S_r}{S_r}\right)^2. \quad (2)$$

For a thin film sample, the relative errors in the reference and sample spectra are largely equal. The relative error in the amplitude transmission spectrum of

a thin film measured with normal THz-TDS can be approximated by

$$\left| \frac{\Delta T}{T} \right|_{\text{TDS}} \approx \sqrt{2} \left| \frac{\Delta S_r}{S_r} \right|. \quad (3)$$

In DTDS, the complex transmission spectrum is calculated from

$$T(\omega) = 1 - \frac{S_d(\omega)}{S_r(\omega)}, \quad (4)$$

where \tilde{S}_d is the complex differential spectrum. Hence

$$\left(\frac{\Delta T}{T} \right)_{\text{DTDS}}^2 \approx \left[\left(\frac{\Delta S_d}{S_d} \right)^2 + \left(\frac{\Delta S_r}{S_r} \right)^2 \right] \left(\frac{S_d}{S_f} \right)^2, \quad (5)$$

where $S_f = S_r - S_d$. Equation 5 shows that using DTDS instead of normal TDS reduces the relative error in the amplitude transmission spectrum by a factor of S_d/S_f , so long as

$$\Delta S_d/S_d \approx \Delta S_f/S_f. \quad (6)$$

Equation (6) is valid for our system dominated by noise in the THz generation arm of the pump-probe system. DTDS is most beneficial for very thin films, where the transmission spectrum of the differential signal S_d is much smaller than the spectra of the film or the reference. The THz phase change induced by a dielectric sample is proportional to its thickness. The improvement in SNR due to DTDS is shown experimentally in Sec. 5 by measuring the reference and differential spectra of a thin film sample.

DTDS was first demonstrated in 2000 to determine the refractive index of a 1.8- μm -thick parylene-N film [51]. This first work developed an analytical expression for the refractive index of the film and dithered the sample at 16 Hz. An improvement on this work was to increase the dither frequency to 66 Hz and thereby reduce the noise in the detected T-rays [54]. Ultrafast lasers have an $1/f$ noise characteristic, so increasing the modulation frequency dramatically reduces noise [44–47]. To increase the modulation frequency further, we use double modulation.

3.2. *Double modulation*

Double modulation is a technique similar to encoding information on a carrier wave in telecommunications. The signal, already modulated at a lower frequency f_2 , is additionally modulated at a higher frequency f_1 by an optical chopper. The frequency f_1 , equivalent to the carrier frequency, is then removed in the detection system through demodulation. The advantage of double modulation is that the noise level is less at the higher modulation frequency, as shown in Fig. 1(b).

The main source of noise in the DTDS experiment is the mode-locked Ti:sapphire laser, with a $1/f$ noise characteristic. Noise can be reduced by modulating the pump beam at some audio or radio frequency f_2 with a mechanical chopper, or an acousto- or electro-optic device. Once converted to an electronic signal with a photo detector of appropriate bandwidth, the depth of the modulation is detected with a lock-in amplifier (LIA). The LIA then passes the signal through a very narrow band filter to

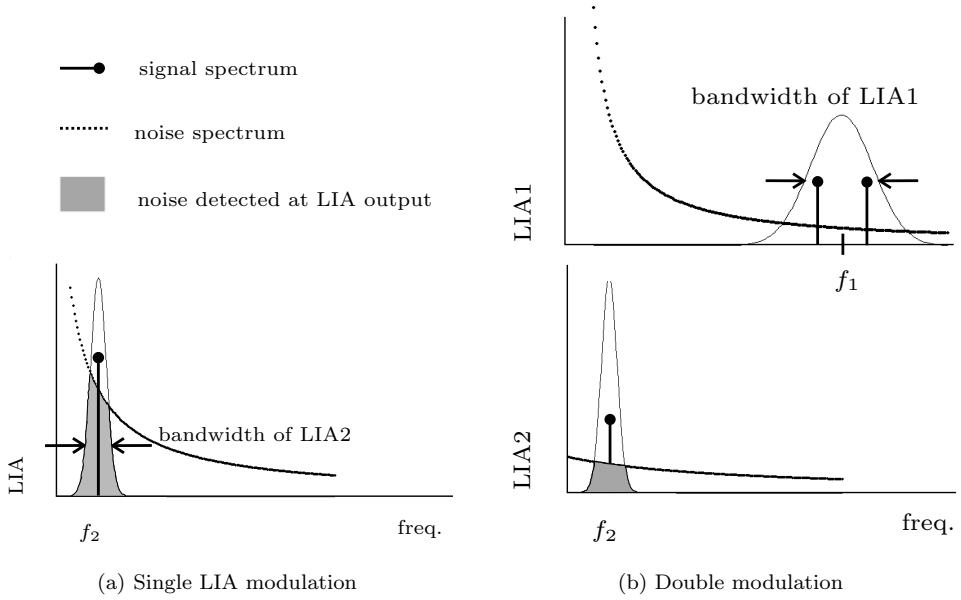


Fig. 2. This figure is a diagrammatic comparison of single and double modulation. (a) shows an experiment with a single LIA. The signal is modulated at a frequency f_2 by, in our case, a galvanometric shaker. Although the signal is chopped by a square wave, the LIA detects the fundamental sine wave, so we consider it to be a single frequency spike. The LIA has a certain bandwidth, set by its time constant, and the noise at the LIA output is determined by the noise power within that bandwidth, which corresponds to the shaded region in Fig. 2(a). (b) demonstrates the operation of double modulation. In double modulation, the signal at the input to the first LIA is found at the sum and difference of the modulation frequencies, $f_1 + f_2$ and $f_1 - f_2$. The first LIA acts as a frequency mixer and demodulates the f_1 frequency, so that at the input of the second LIA, the signal is modulated at f_2 . The advantage of DTDS is that the noise found at the output of the second LIA is far less than in the single LIA setup. One important point is that the bandwidth of the first LIA has to be set sufficiently wide to allow the signal to pass through at a frequency $\pm f_2$ from the center frequency. Double modulation can be achieved using a LIA driven by a synthesized frequency $f_1 + f_2$, unless the sum frequency is at radio frequencies (RF). In that case, it is advantageous to have the second LIA operating at audio frequencies (AF) because an AF LIA has better operating characteristics than an RF LIA [55].

reject any variations not at the modulation frequency. Single frequency modulation is diagrammatically described in Fig. 2(a). The important quantity is the shaded area under the noise curve, which indicates the amount of noise appearing at the output of the LIA.

Ideally an experiment should be modulated at as high a frequency as possible. For mode-locked lasers, $1/f$ signal fluctuations dominate at frequencies below 3 MHz, where the shot noise limit is reached [56]. As discussed in Sec. 4, we have used a galvanometric scanner as the second modulator, and it is impossible to shake the thin film sample above audio frequencies because of mechanical inertia. Galvanometric scanners do not have sufficient travel at frequencies above 100 Hz when a sample is attached. At modulation frequencies below 100 Hz, the $1/f$ noise levels are very high, greatly reducing the sensitivity of DTDS. Double modulation enables the use of an high carrier frequency, which sets the noise level, and an arbitrarily low

shaker frequency. Galvanometer operation at a frequency less than 20 Hz, where $1/f$ noise is very high, eliminates heating problems and enables a larger shaking amplitude. The process of double modulation and demodulation is shown in Fig. 2(b). The narrow detection bandwidth of LIA2 at f_2 rejects any harmonics caused by double modulation.

A schematic layout of double modulation as implemented in our experiment is shown in Fig. 3. The pump beam is first modulated at f_1 by the mechanical chopper and then modulated at f_2 by the dithered thin film sample. The double modulated T-ray signal is converted to a polarization modulation of the probe beam using electro-optic detection [22]. Balanced PDs detect the polarization modulation of the probe beam, and the first LIA, acting as a mixer, demodulates the chopper f_1 . The second LIA detects the thin film signal at f_2 and provides a complex output representing the DTDS waveform at a given pump-probe delay. The delay is scanned to sample the entire T-ray waveform.

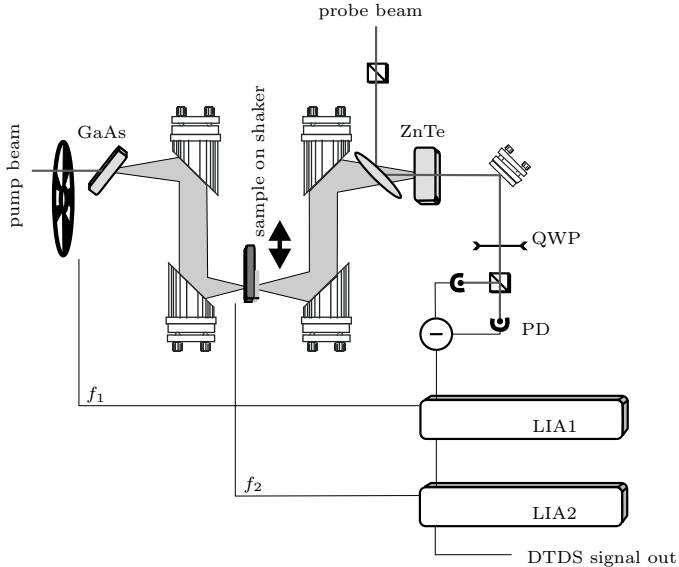


Fig. 3. Schematic of the DTDS experiment. The pump and probe beams are split from the ultrafast laser. This experimental setup is explained in Sec. 4.

To quantify the improvement in SNR due to double modulation, we have to consider both the decrease in noise level and the decrease in signal level it causes. Modulating the signal with a second modulator decreases its amplitude by half. Each modulator blocks fifty percent of the pump beam. If, however, the reduction in noise is better than fifty percent, then double modulation results in an improved SNR. In Fig. 1(b) we show the noise spectrum of our T-ray system, which uses balanced photodiode (PD) detection [57, 58]. If the modulation frequency is set to 3 kHz or higher, the noise level drops by an order of magnitude compared to a modulation frequency of 100 Hz or lower. This is the improvement that we predict for a system dominated by $1/f$ noise.

4. Experimental Setup

Our T-ray system is a typical system, using a semiconductor T-ray source and electro-optic detection [59–61].

The optical layout is shown in Fig. 3. Our ultrafast laser is a Spectra-Physics Tsunami Ti:sapphire oscillator, multi-line pumped by a Spectra-Physics BeamLoc large frame argon-ion laser, and producing 1.7 W average power of 100-fs pulses at an 82-MHz repetition rate [62]. Our pump beam power is about 800 mW after passing through a mechanical chopping wheel, which modulates the beam at f_1 . T-rays are generated by ultrafast current transients in a thin GaAs wafer mounted at Brewster’s angle to the beam. The T-rays are collimated and focused with off-axis gold-coated paraboloidal reflectors, and detected in a collinear geometry in a 2-mm-thick $\langle 110 \rangle$ -oriented ZnTe crystal. The probe beam power is approximately 100 mW and we detect 1 mA of current in each of the balanced PDs. The polarization rotation of the probe beam is detected by a Wollaston analyzer and balanced PDs. A quarter wave plate (QWP) is used to compensate for the intrinsic birefringence in the ZnTe. The difference current from the PDs, proportional to the T-ray electric field, is filtered by two LIAs, as described in Sec. 3.2. The first LIA has a time constant of 300 μ s, which corresponds to a 260-Hz filter bandwidth, and the second LIA has a time constant of 100 ms.

The thin film sample is held in a galvanometric shaker from Cambridge Technology [63], operating at f_2 . The shaker itself is mounted in a large aluminium heat sink to keep its operating temperature below 50°C. The heat sink, despite its proximity to the T-ray beam path, has less than 1% effect on the transmitted T-ray waveforms. The diameter of the T-ray spot on the sample is less than 2 mm.

The thin film sample used in these experiments is a rectangle of amorphous glass, half-covered with a 180- μ m-thick layer of black electrical tape. A relatively thick film is used to demonstrate the reduction of noise in DTDS compared to TDS; if a film is too thin, no results is observed in TDS. The glass slide is approximately 30-mm high, 13-mm wide and 1-mm thick. A sample this size ensures the THz beam passes wholly and exclusively through either the sample or the substrate as it oscillates. The sample was driven sinusoidally at 5 Hz. A low frequency allows the galvanometer to operate with a large amplitude and without over-heating.

5. Results and Discussion

The raw time domain data from a DTDS experiment are shown in Fig. 4(a). Even for a relatively thick 180- μ m film, the difference between the waveforms propagated through the substrate and through the film is almost indistinguishable. The differential signal is far smaller than the other waveforms, and is 90° out of phase with the reference waveform. The DTDS technique was first called *differential* because the DTDS signal is an approximate differentiation of the reference signal with respect to time; the optical delay caused by the moving the thin film into the beam path is a very small Δt . By measuring the small change in amplitude of the transmitted signal, Δy , and plotting as a function of time delay, one is approximately measuring the slope of the reference waveform, dy/dt .

The amplitude spectra of the reference and differential waveforms are plotted in Fig. 4(b). The 0.2 to 2 THz bandwidth of the reference pulse is typical for this

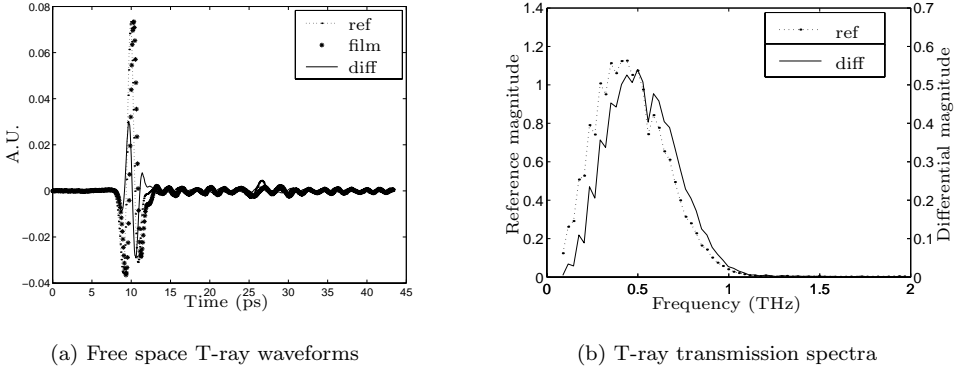


Fig. 4. Experimental T-ray time-domain waveforms and spectra. (a) shows the reference waveform through the substrate, the waveform through the film, and the differential signal. These measurements were taken with a LIA time constant of 100 ms, at room temperature. (b) shows the transmission spectra of the reference and differential T-ray waveforms. Phase information is linear and is not shown in these plots. The bandwidth of the reference pulse is typical for our T-ray system, driven as it is by T-ray generation from a GaAs surface using 100-fs optical pulses. The absorption lines at 0.56, 0.75 and 1.1 THz are caused by water vapor in the air [53].

100-fs laser T-ray system. The strong absorption lines are due to water vapor in the air [53]. The water lines are removed in the deconvolution process, but still result in a lower SNR at affected frequencies. The differential signal has a reduced bandwidth because decreased SNR, although the approximate shape is the same as the reference spectrum.

The noise level in these measurements can be estimated experimentally with repeated measurements. Each experiment is repeated four times over a day to estimate the uncertainty. The experimental errors for TDS and DTDS are summarized in Table 2. As detailed in the figure caption, the observed noise is less than expected because the noise in each waveform is correlated to some extent. The noise values for DTDS are larger than TDS because we have used double modulation, which halves the signal, and contains noise introduced by the galvanometer.

Table 1. Comparison of equations for estimating the experimental error in measured transmission coefficients in THz-TDS and DTDS. DTDS has an inherently lower noise level than TDS by a factor of approximately $|\tilde{S}_d|/|\tilde{S}_r|$, the ratio of the differential and reference spectra. For thin films, where the sample and reference spectra are substantially similar, the ratio $|\tilde{S}_d|/|\tilde{S}_r|$ is far less than unity, so noise in DTDS is less than in TDS.

	MEASURE	$ \Delta T/T $
TDS	$ \Delta S_r $ $ S_r $	$\sqrt{2} \left \frac{\Delta S_r}{S_r} \right $
DTDS	$ \Delta S_d $ $ S_d $	$\sqrt{2} \left \frac{\Delta S_r}{S_r} \right \left \frac{S_d}{S_r} \right $

Table 2. This table shows calculated and observed measurement fluctuations for the 0.5-THz frequency component of the reference, differential and transmission spectra. The fluctuation level at 0.5 THz was chosen because it is close to the peak of the frequency spectrum (Fig. 4(b)). The measured errors were determined from the spread of four repeated measurements under identical conditions. The raw error in DTDS is much larger than for TDS for two main reasons: firstly, this data was taken with double modulation, so the signal level is half that in TDS. Secondly, there is noise inherent in the galvanometer system, which we expect contributes to measurement fluctuations. The calculated $|\Delta T/T|$ are estimated using the equation in Table 1 for TDS and from Eq. (5) for DTDS. Equation (5) must be used because, in this experiment, the condition expressed in Eq. (6) does not hold. The observed $|\Delta T/T|$ were determined from four numerical calculations of the transmission amplitude at 0.5 THz. The observed values are both less than the expected values. This is most likely due to our assumption of uncorrelated noise in successive measurements. The measurement to measurement fluctuations for the reference, sample and differential waveforms is correlated to some extent, so there is an element of noise cancelation in the deconvolution calculation that determines \bar{T} .

	MEASURE	Calculated $ \Delta T/T $	Observed $ \Delta T/T $
TDS	$\left \frac{\Delta S_r}{S_r} \right = 1.0\%$	1.4%	1.0%
DTDS	$\left \frac{\Delta S_d}{S_d} \right = 4.6\%$	2.4%	1.4%

The results of this experiment demonstrate the accuracy of the DTDS technique, and confirm the estimates of noise reduction from thin film samples.

Figure 5 shows the noise spectrum of the T-ray system, and demonstrates the benefits of using double-modulated DTDS (d-DTDS) over “normal” DTDS (n-DTDS). This spectrum was measured using a modulator and a lock-in amplifier at values of frequency, increasing from 2 Hz to 2 kHz. The galvanometer (“galvo”) was used to measure noise from 2 to 10 Hz and an optical chopper (“chopper”) was used for 10 Hz to 2 kHz. Each set of measurements has two values, which are upper and lower bounds indicating the approximate errors in the measurements. For these values the delay stage (see Fig. 3) was set at the pulse peak (Fig. 4(a)), and each noise value was measured using the lock-in amplifier, resulting in root-mean-squared noise value found at the peak of the T-ray signal pulse. The measured noise value from the LIA was normalized to the actual value of the T-ray peak, to account for very slow laser fluctuations, and to the bandwidth of the LIA low-pass filter — this value can be considered an *inverse* signal-to-noise ratio. There is a clear discrepancy between the noise level of the chopper modulation and the galvanometer modulation. This noise increase is due to the physical instabilities in the galvanometer and slight fluctuations in its modulation frequency. This problem could be reduced by engineering a better shaker and drive circuitry.

Figure 5 compares the measured noise spectrum to a $1/f$ trend, which is typical of laser noise spectra [44]. System noise measured under chopper modulation corresponds well to this relationship, until it is driven at higher frequencies, above 500 Hz. The optical chopper used in this experiment has an operational limit of 6 kHz, and at the higher operating frequencies starts to introduce additional noise into the system. This can be avoided by using a modulator designed for higher frequency operation, such as an acousto-optic modulator.

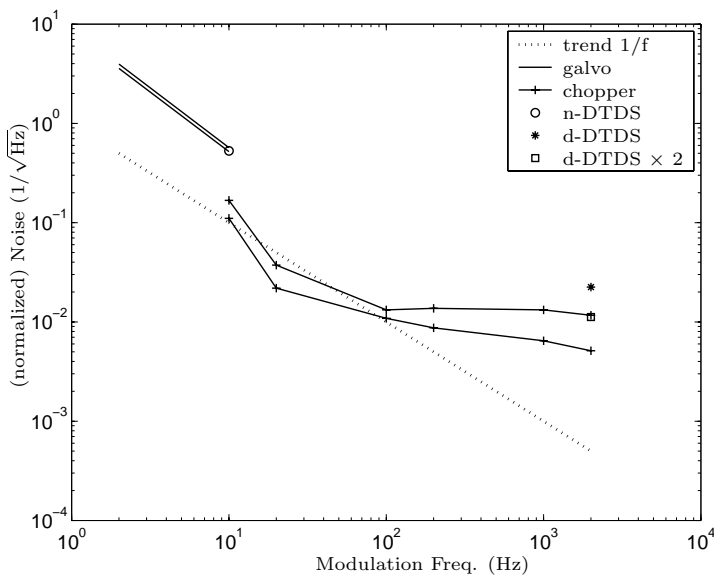


Fig. 5. Experimental noise spectrum of the T-ray system for increasing modulation frequency, showing the noise reduction due to double modulation. The noise spectrum measured with the galvanometer and the optical chopper are compared to a theoretical $1/f$ trend, which is typical of experiments dominated by laser noise. The measured noise spectra are represented by two lines, which are the upper and lower bounds of the error bounds for each measurement, and are normalized to the signal strength (in effect this is a plot of the inverse signal-to-noise ratio). Both modulators show noise spectra with the $1/f$ trend, except the noise level with galvanometer modulation is larger, due to mechanical instabilities and jitter in the shaking frequency. The noise levels of experiments using normal (one LIA) DTDS and double-modulated DTDS are shown as points on the spectrum. The value “n-DTDS $\times 2$ ” is *half* the actual noise of the d-DTDS experiment. This point is shown to demonstrate that, had the signal level not been halved by the dual modulators, the experimental noise would fit on the spectral curve as expected.

Lastly, Fig. 5 shows the noise levels of normal DTDS (“n-DTDS”) compared to double-modulated DTDS (“d-DTDS”). The reduction in noise due to double modulation is evident, and clearly due to the second higher modulation frequency. Double modulation reduces noise due to the galvanometer instability and due to low-frequency laser fluctuations. This reduction in noise is approximately predicted by the $1/f$ noise trend typical of systems dominated by laser noise. “d-DTDS $\times 2$ ” is shown to indicate what the normalized noise value would be if the signal strength in d-DTDS were doubled. “d-DTDS” suffers a reduction in signal strength by half, as mentioned above.

Our results show that noise is greatly reduced in T-ray thin-film measurements when using a double-modulated differential system.

6. Conclusions and Future Directions

We have demonstrated the application of double modulation to improve the SNR of DTDS of thin films by over an order of magnitude. DTDS has been presented as a method of overcoming the difficulty of T-ray spectroscopy of thin films by

reducing the effects of noise. This improvement has been quantified mathematically. DTDS can be improved by using double modulation, which has been explained and implemented experimentally. Our experimental results demonstrate the noise reduction due to DTDS, which makes it possible to detect thin films with T-rays, and the further improvement due to double modulation (d-DTDS). This simple technique enables thin films to be characterized in the GHz-THz range for fast integrated circuit technology, and for novel work in far-infrared biosensor systems.

There are a number of system improvements and potential applications that remain to be explored in DTDS. We expect that the noise of the system can be further reduced by using a modulation frequency higher than 3 kHz, coupled with an RF LIA.

We will be applying the DTDS method to characterize thin biomolecular films for lab-on-a-chip applications. It will be valuable to be able to non-invasively probe the hydration, conformation and activity of protein films used, for example, as enzyme catalysts layered on inorganic substrates. DTDS is an ideal technique for such research.

Acknowledgments

Samuel Mickan would like to acknowledge the support of the Fulbright Commission and Clough Engineering (Australia). This work was funded in part by the U. S. National Science Foundation, the U. S. Army Research Office and the Australian Research Council (ARC).

References

- [1] S. P. Mickan, D. Abbott, J. Munch and X.-C. Zhang, *Double modulated differential THz-TDS for thin film dielectric characterization*, *Microelectronics Journal* **Submitted** (2002).
- [2] M. L. Green, E. P. Gusev, R. Degraeve and E. L. Garfunkel, *Ultrathin (< 4 nm) SiO₂ and Si-O-N gate dielectric layers for silicon microelectronics: Understanding the processing, structure, and physical and electrical limits*, *Journal of Applied Physics* **90**(5) (2001) 2057–2121.
- [3] A. I. Kingon, J.-P. Maria and S. K. Streiffer, *Alternative dielectrics to silicon dioxide for memory and logic devices*, *Nature* **406**(6779) (2000) 1032–1038.
- [4] C. R. Kagan, D. B. Mitzi and C. D. Dimitrakopoulos, *Organic-inorganic hybrid materials as semiconducting channels in thin-film field-effect transistors*, *Science* **286**(5441) (1999) 945–947.
- [5] C. D. Dimitrakopoulos, S. Purushothaman, J. Kymissis, A. Callegari and J. Shaw, *Low-voltage organic transistors on plastic comprising high-dielectric constant gate insulators*, *Science* **283**(5403) (1999) 822–824.
- [6] F.-J. Meyer zu Heringdorf, M. C. Reuter and R. M. Tromp, *Growth dynamics of pentacene thin films*, *Nature* **412**(6846) (2001) 517–520.
- [7] M. Brucherseifer, P. Haring Bolívar, H. Klingenberg and H. Kurz, *Angle-dependent THz tomography — characterization of thin ceramic oxide films for fuel cell applications*, *Applied Physics B: Lasers and Optics* **72**(3) (2001) 361–366.
- [8] M. C. Nuss and J. Orenstein, *Terahertz time-domain spectroscopy*, in *Millimeter and submillimeter wave spectroscopy of solids*, Vol. 74 of *Topics in Applied Physics*, Ch. 2, pp. 7–50, ed. G. Grüner, Springer-Verlag, Berlin, Germany (1998).

- [9] B. Lax, *Applications of far infrared lasers*, in *Tunable Lasers and Applications*, Vol. 3 of *Springer Series in Optical Sciences*, pp. 340–347, eds. A. Mooradian, T. Jaeger and P. Stokseth, Springer-Verlag, Berlin (1976).
- [10] S. P. Mickan, D. Abbott, J. Munch, X.-C. Zhang and T. van Doorn, *Analysis of system trade-offs for terahertz imaging*, *Microelectronics Journal* **31**(7) (2000) 503–514.
- [11] P. Y. Han, M. Tani, M. Usami, S. Kono, R. Kersting and X.-C. Zhang, *A direct comparison between terahertz time-domain spectroscopy and far-infrared Fourier transform spectroscopy*, *Journal of Applied Physics* **89**(4) (2001) 2357–2359.
- [12] E. Bründermann, D. R. Chamberlin and E. Haller, *Novel design concepts of widely tunable germanium terahertz lasers*, *Infrared Physics and Technology* **40**(3) (1999) 141–151.
- [13] M. Jackson, E. M. Telles, M. D. Allen and K. M. Evenson, *Short-wavelength far-infrared laser cavity yielding new laser emissions in CD_3OH* , *Applied Physics B: Lasers and Optics* **72**(7) (2001) 815–818.
- [14] S. S. Dhillon, A. G. Davies, R. Harrell, E. H. Linfield, D. A. Ritchie, M. Pepper and D. D. Arnone, *Terahertz (THz) electro-luminescence from AlGaAs-GaAs quantum cascade heterostructures*, in *Conference on Lasers and Electro-Optics '01*, Baltimore, MD, U.S.A. (May 2001) IEEE LEOS & OSA, 483–484.
- [15] A. Pimenov, A. V. Pronin, A. Loidl, A. P. Kampf, S. I. Krasnovobodtsev and V. S. Nozdrin, *Submillimeter spectroscopy of tilted $Nd_{1.85}Ce_{0.15}CuO_{4-\delta}$ films: Observation of a mixed ac-plane excitation*, *Applied Physics Letters* **77**(3) (2000) 429–431.
- [16] D. H. Auston and M. C. Nuss, *Electrooptic generation and detection of femtosecond electrical transients*, *IEEE Journal of Quantum Electronics* **24**(2) (1988) 184–197.
- [17] J. A. Valdmanis, G. A. Mourou and C. W. Gabel, *Subpicosecond electrical sampling*, *IEEE Journal of Quantum Electronics* **19**(4) (1983) 664–667.
- [18] M. Y. Frankel, J. F. Whitaker and G. A. Mourou, *Optoelectronic transient characterization of ultrafast devices*, *IEEE Journal of Quantum Electronics* **28**(10) (1992) 2313–2324.
- [19] D. H. Auston and K. P. Cheung, *Coherent time-domain far-infrared spectroscopy*, *Journal of the Optical Society of America B: Optical Physics* **2**(4) (1985) 606–612.
- [20] C. Fattinger and D. Grischkowsky, *Point source terahertz optics*, *Applied Physics Letters* **53**(16) (1988) 1480–1482.
- [21] B. B. Hu, X.-C. Zhang and D. H. Auston, *Free-space radiation from electro-optic crystals*, *Applied Physics Letters* **56**(6) (1990) 506–508.
- [22] Q. Wu and X.-C. Zhang, *Free-space electro-optic sampling of terahertz beams*, *Applied Physics Letters* **67**(24) (1995) 3523–3525.
- [23] Y. Pastol, G. Arjavalingham, J.-M. Halbout and G. V. Kopschay, *Coherent broadband microwave spectroscopy using picosecond optoelectronic antennas*, *Applied Physics Letters* **54**(4) (1989) 307–309.
- [24] D. Grischkowsky, S. Keiding, M. van Exter and C. Fattinger, *Far-infrared time-domain spectroscopy with terahertz beams of dielectrics and semiconductors*, *Journal of the Optical Society of America B: Optical Physics* **7**(10) (1990) 2006–2015.
- [25] B. B. Hu and M. C. Nuss, *Imaging with terahertz waves*, *Optics Letters* **20**(16) (1995) 1716–1718.
- [26] D. M. Mittleman, M. Gupta, R. Neelamani, R. G. Baraniuk, J. V. Rudd and M. Koch, *Recent advances in terahertz imaging*, *Applied Physics B: Lasers and Optics* **68**(6) (1999) 1085–1094.
- [27] Z. Jiang, X. G. Xu and X.-C. Zhang, *Improvement of terahertz imaging with a dynamic subtraction technique*, *Applied Optics* **39**(17) (2000) 2982–2987.

- [28] Q. Chen, M. Tani, Z. Jiang and X.-C. Zhang, *Electro-optic transceivers for terahertz-wave applications*, *Journal of the Optical Society of America B: Optical Physics* **18**(6) (2001) 823–831.
- [29] A. B. Ruffin, J. Decker, L. Sanchez-Palencia, L. Le Hors, J. F. Whitaker, T. B. Norris and J. Van Rudd, *Time reversal and object reconstruction with single-cycle pulses*, *Optics Letters* **26**(10) (2001) 681–683.
- [30] B. Ferguson, S. Wang and X.-C. Zhang, *T-ray computed tomography*, in *IEEE/LEOS Annual Meeting Conference Proceedings*, Vol. 1. IEEE, San Diego, CA, U.S.A. (Nov. 2001) PD1.7–PD1.8.
- [31] Q. Chen, Z. Jiang, G. X. Xu and X.-C. Zhang, *Near-field terahertz imaging with a dynamic aperture*, *Optics Letters* **25**(15) (2000) 1122–1124.
- [32] O. Mitrofanov, I. Brener, M. C. Wanke, R. R. Ruel, J. D. Wynn, A. J. Bruce and J. Federici, *Near-field microscope probe for far infrared time domain measurements*, *Applied Physics Letters* **77**(4) (2000) 591–3.
- [33] O. Mitrofanov, I. Brener, R. Harel, J. D. Wynn, L. N. Pfeiffer, K. W. West and J. Federici, *Terahertz near-field microscopy based on a collection mode detector*, *Applied Physics Letters* **77**(22) (2000) 3496–8.
- [34] R. A. Cheville and D. Grischkowsky, *Time domain terahertz impulse ranging studies*, *Applied Physics Letters* **67**(14) (1995) 1960–1962.
- [35] Z. G. Lu, P. Campbell and X.-C. Zhang, *Free-space electro-optic sampling with a high-repetition-rate regenerative amplified laser*, *Applied Physics Letters* **71**(5) (1997) 593–595.
- [36] R. M. Woodward, B. Cole, V. P. Wallace, D. D. Arnone, R. Pye, E. H. Linfield, M. Pepper and A. G. Davies, *Terahertz pulse imaging of in-vitro basal cell carcinoma samples*, in Conference on Lasers and Electro-Optics '01, Baltimore, MD, U.S.A. (May 2001) IEEE LEOS & OSA,329–330.
- [37] M. Li, G. C. Cho, T.-M. Lu, X.-C. Zhang, S.-Q. Wang and J. T. Kennedy, *Time-domain dielectric constant measurement of thin film in GHz-THz frequency range near Brewster angle*, *Applied Physics Letters* **74**(15) (1999) 2113–2115.
- [38] M. Tonouchi, M. Yamashita and M. Hangyo, *Vortex penetration in YBCO thin film strips observed by THz radiation imaging*, *Physica B* **284–288** (2000) 853–854.
- [39] D. R. Grischkowsky, *Optoelectronic characterization of transmission lines and waveguides by terahertz time-domain spectroscopy*, *IEEE Journal of Selected Topics in Quantum Electronics* **6**(6) (2000) 1122–1135.
- [40] G. Gallot, S. P. Jamison, R. W. McGowan and D. Grischkowsky, *Terahertz waveguides*, *Journal of the Optical Society of America B: Optical Physics* **17**(5) (2000) 851–863.
- [41] M. Brucherseifer, M. Nagel, P. Haring Bolívar, H. Kurz, A. Bosserhoff and R. Büttner, *Label-free probing of the binding state of DNA by time-domain terahertz sensing*, *Applied Physics Letters* **77**(24) (2000) 4049–4051.
- [42] M. Ree, K.-J. Chen, D. P. Kirby, N. Katzenellenbogen and D. Grischkowsky, *Anisotropic properties of high-temperature polyimide thin films: Dielectric and thermal-expansion behaviors*, *Journal of Applied Physics* **72**(5) (1992) 2014–2021.
- [43] L. Duvillaret, F. Garet and J.-L. Coutaz, *A reliable method for extraction of material parameters in terahertz time-domain spectroscopy*, *IEEE Journal of Selected Topics in Quantum Electronics* **2**(3) (1996) 739–746.
- [44] D. von der Linde, *Characterization of the noise in continuously operating mode-locked lasers*, *Applied Physics B: Photophysics and Laser Chemistry* **39**(4) (1986) 201–217.
- [45] H. A. Haus and A. Mecozzi, *Noise of mode-locked lasers*, *IEEE Journal of Quantum Electronics* **29**(3) (1993) 983–996.

- [46] J. Son, J. V. Rudd and J. F. Whitaker, *Noise characterization of a self-mode-locked Ti:sapphire laser*, *Optics Letters* **17**(10) (1992) 733–735.
- [47] A. Poppe, L. Xu, F. Krausz and C. Spielmann, *Noise characterization of sub-10-fs Ti:sapphire oscillators*, *IEEE Journal of Selected Topics in Quantum Electronics* **4**(2) (1998) 179–184.
- [48] J. L. Johnson, T. D. Dorney and D. M. Mittleman, *Enhanced depth resolution in terahertz imaging using phase-shift interferometry*, *Applied Physics Letters* **78**(6) (2001) 835–837.
- [49] S. Krishnamurthy, M. T. Reiten, S. A. Harmon and R. A. Cheville, *Characterization of thin polymer films using terahertz time-domain interferometry*, *Applied Physics Letters* **79**(6) (2001) 875–7.
- [50] M. Nagel, P. Haring Bolívar, M. Brucherseifer, H. Kurz, A. Bosserhoff and R. Büttner, *Integrated THz technology for label-free genetic diagnostics*, *Applied Physics Letters* **80**(1) (2002) 154–156.
- [51] Z. Jiang, M. Li and X.-C. Zhang, *Dielectric constant measurement of thin films by differential time-domain spectroscopy*, *Applied Physics Letters* **76**(22) (2000) 3221–3223.
- [52] M. Brucherseifer, H. P. M. Pellemans, P. Haring Bolívar and H. Kurz, *THz spectroscopy with ultrahigh sensitivity*, in Conference on Lasers and Electro-Optics '00, San Francisco, CA, U.S.A. (May 2000) IEEE LEOS & OSA, 553–554.
- [53] M. van Exter, C. Fattinger and D. Grischkowsky, *Terahertz time-domain spectroscopy of water vapor*, *Optics Letters* **14**(20) (1989) 1128–1130.
- [54] K.-S. Lee, J. Y. Kim, J. Fortin, Z. Jiang, M. Li, T.-M. Lu and X.-C. Zhang, *Dielectric property measurement of sub-micron thin films by differential time-domain spectroscopy*, in *Ultrafast Phenomena XII*, Vol. 66 of *Springer Series in Chemical Physics*, pp. 232–234, eds. T. Elsaesser, S. Mukamel, M. M. Murnane and N. F. Scherer, Springer-Verlag, Berlin (2000).
- [55] S. V. Frolov and Z. V. Vardeny, *Double-modulation electro-optic sampling for pump-and-probe ultrafast correlation measurements*, *Review of Scientific Instruments* **69**(3) (1998) 1257–1260.
- [56] L. Andor, A. Lőrincz, J. Siemion, D. D. Smith and S. A. Rice, *Shot-noise-limited detection scheme for two-beam laser spectroscopies*, *Review of Scientific Instruments* **55**(1) (1984) 64–67.
- [57] B. R. Hemenway, H. K. Heinricn, J. H. Goll, Z. Xu and D. M. Bloom, *Optical detection of charge modulation in silicon integrated circuits using a multimode laser-diode probe*, *IEEE Electron Device Letters* **8**(8) (1987) 344–346.
- [58] J. M. Zhang, R. L. Ruo and M. K. Jackson, *Noise suppression in Ti:sapphire laser-based electro-optic sampling*, *Applied Physics Letters* **75**(22) (1999) 3446–3448.
- [59] Z. Jiang and X.-C. Zhang, *Terahertz imaging via electrooptic effect*, *IEEE Transactions on Microwave Theory and Techniques* **47**(12) (1999) 2644–2650.
- [60] X.-C. Zhang, B. B. Hu, J. T. Darrow and D. H. Auston, *Generation of femtosecond electromagnetic pulses from semiconductor surfaces*, *Applied Physics Letters* **56**(11) (1990) 1011–1013.
- [61] M. Li, F. G. Sun, G. A. Wagoner, M. Alexander and X.-C. Zhang, *Measurement and analysis of terahertz radiation from bulk semiconductors*, *Applied Physics Letters* **67**(1) (1995) 25–27.
- [62] <http://www.spectra-physics.com/>.
- [63] <http://www.camtech.com/>.